



Coincidence of Homeostasis and Bifurcation in Feedforward Networks

William Duncan

*Department of Mathematics, Duke University,
Durham, NC 27708, USA
wduncan@math.duke.edu*

Martin Golubitsky

*Department of Mathematics, The Ohio State University,
Columbus, OH 43210, USA
golubitsky.4@osu.edu*

Received April 25, 2019

Homeostasis is an important and common biological phenomenon wherein an output variable does not change very much as an input parameter is varied over an interval. It can be studied by restricting attention to homeostasis points — points where the output variable has a vanishing derivative with respect to the input parameter. In a feedforward network, if a node has a homeostasis point then downstream nodes will inherit it. This is the case except when the downstream node has a bifurcation point coinciding with the homeostasis point. We apply singularity theory to study the behavior of the downstream node near these homeostasis-bifurcation points. The unfoldings of low codimension homeostasis-bifurcation points are found. In the case of steady-state bifurcation, the behavior includes multiple homeostatic plateaus separated by hysteretic switches. In the case of Hopf bifurcation, the downstream node may have limit cycles with a wide range of near-constant amplitudes and periods. Homeostasis-bifurcation is therefore a mechanism by which binary, switch-like responses or stable clock rhythms could arise in biological systems.

Keywords: Homeostasis; bifurcation; biochemical networks; singularity theory.

1. Introduction

Homeostasis and bifurcation are common behaviors in dynamical systems that depend on a parameter. Homeostasis occurs when the output of a system is approximately constant on an interval of the (input) parameter. Bifurcation occurs when the number or type of solutions change as a (bifurcation) parameter is varied. Local bifurcation occurs at an equilibrium when the Jacobian of the system has an eigenvalue with zero real part as the bifurcation parameter varies. Analogously it is shown in

[Golubitsky & Stewart, 2016] that homeostasis can be studied by restricting attention to infinitesimal homeostasis points — single points where a component of the system has a vanishing derivative with respect to a parameter — rather than homeostatic intervals. Under this formulation, homeostasis is treated as a singularity of the system. This theory has been used to find homeostatic plateaus in gene regulatory networks [Antoneli *et al.*, 2018] and to explain a paradoxical response in asthma treatment [Donovan, 2018].

1.1. Homeostasis singularities

Consider the differential equation $\dot{X} = G(X, \lambda)$ where $X \in \mathbb{R}^m$ and $\lambda \in \mathbb{R}$ is a parameter. We assume there is a stable equilibrium at $(X, \lambda) = (0, 0)$. We may then apply the implicit function theorem to $G(X, \lambda) \equiv 0$ to obtain a curve of stable equilibria as a function of λ , say $X(\lambda)$ where $X(0) = 0$. In applications, we are concerned with the homeostatic properties of a distinguished variable x that we define to be X_i for some i . We call $x(\lambda)$ the input–output function and note that it has an *infinitesimal homeostasis* point at $\lambda = 0$ if $x'(0) = 0$. Consecutive higher-order derivatives may also vanish at the origin, increasing the codimension of the singularity of $x(\lambda)$. We will use $\text{codim}_H(x)$ to denote the codimension of $x(\lambda)$ as a homeostasis point. As codimension increases, we expect the input–output function to be approximately constant on a wider interval and therefore more homeostatic, but low codimension phenomena are more common.

Singularity theory studies the structure of singularities and their perturbations up to appropriate changes of coordinates. It is shown in [Golubitsky & Stewart, 2016] that the appropriate changes of coordinates for homeostasis are those of elementary catastrophe theory. The normal forms for the singularities and their universal unfoldings are reviewed in that paper. The codimension of a singularity is the number of parameters that are found in a universal unfolding of that singularity. The universal unfoldings of the codimension 0 and 1 homeostasis points are listed in Table 1.

1.2. Bifurcation singularities

We consider bifurcation points with a distinguished bifurcation parameter. Consider a system of the form $\dot{Y} = F(Y, \mu)$, where $Y \in \mathbb{R}^n$ and $\mu \in \mathbb{R}$ is the bifurcation parameter. We assume that F

Table 1. Universal unfoldings of codimension 0 and 1 infinitesimal homeostasis points.

Input–Output Function, $x(\lambda)$	Nomenclature	$\text{codim}_H(x)$
$\varepsilon\lambda^2$	Simple homeostasis	0
$\varepsilon\lambda^3 + a_1\lambda$	Chair	1

where $\varepsilon = \pm 1$. The normal form for the chair may be recovered by setting $a_1 = 0$. The universal unfolding of simple homeostasis is itself.

Table 2. Universal unfoldings of low codimension bifurcation points.

Bifurcation Problem, $f(y, \mu)$	Nomenclature	$\text{codim}_B(f)$
Steady-state bifurcations		
$\varepsilon y^2 + \delta\mu$	Limit point	0
$\varepsilon(y^2 - \mu^2 + b)$	Simple bifurcation	1
$\varepsilon(y^2 + \mu^2 + b)$	Isola	1
$\varepsilon y^3 + \delta\mu + by$	Hysteresis	1
Hopf bifurcations		
$\varepsilon y^3 + \delta y\mu$	Simple Hopf	0
$\varepsilon(y^3 + y\mu^2 + by)$	Isola Hopf	1
$\varepsilon(y^3 - y\mu^2 + by)$		1
$\varepsilon y^5 + \delta y\mu + by^3$		1

where $\varepsilon = \pm 1$ and $\delta = \pm 1$. The normal forms of codimension 1 bifurcations can be recovered by setting $b_1 = 0$. The universal unfolding of a codimension 0 bifurcation is itself.

undergoes a simple 0-eigenvalue steady-state bifurcation or a simple $\pm i\omega$ eigenvalue Hopf bifurcation at the origin. It is shown in [Golubitsky & Schaeffer, 1985] that either case leads to a scalar equation $f(y, \mu) = 0$, $y \in \mathbb{R}$, whose solutions are in one-to-one correspondence with equilibria of the full system in the case of steady-state bifurcation or to amplitudes of limit cycles in the case of Hopf bifurcation. We denote the codimension of a bifurcation point by $\text{codim}_B(f)$. The universal unfoldings of the codimension 0 and 1 bifurcation points are listed in Table 2.

1.3. Combined homeostasis and bifurcation singularities

Given the ubiquity of homeostasis and bifurcation, it is natural to study the behavior of systems where the two singularities coexist. However, homeostasis points require the existence of an input–output function, which is not well defined at bifurcation points. We resolve this problem by assuming a feedforward network structure in which the input–output function of a homeostatic system is substituted for the bifurcation parameter in a bifurcating system.

The first equation in the system has the form

$$\dot{X} = G(X, \lambda), \quad (1)$$

where $X \in \mathbb{R}^m$ and $x \equiv X_i \in \mathbb{R}$ is the distinguished, homeostatic variable of (1) as a function of $\lambda \in \mathbb{R}$.

The second equation in the system has the form

$$\dot{Y} = F(Y, x), \quad (2)$$

where $Y \in \mathbb{R}^n$. Next suppose $x(\lambda)$ has a homeostasis point at λ_0 (that is, $x'(\lambda_0) = 0$) and $x(\lambda_0) = x_0$. Suppose also that $F(Y_0, x_0) = 0$, but F does not have a steady-state bifurcation at (Y_0, x_0) . Then we may apply the implicit function theorem to obtain a curve of equilibria $Y(x(\lambda)) \in \mathbb{R}^n$ for (2) when λ is near λ_0 . Differentiating at λ_0 , we have

$$\frac{d}{d\lambda} Y(x(\lambda)) \Big|_{\lambda=\lambda_0} = \frac{dx}{d\lambda}(\lambda_0) \frac{dY}{dx}(x_0) = 0 \quad (3)$$

so that all Y variables inherit homeostasis points from x . If F has a bifurcation point, one could vary parameters so that the inherited homeostasis and bifurcation points coincide.

We call points λ_0 where infinitesimal homeostasis points $x(\lambda_0)$ coincide with bifurcation points in $F(Y, x)$ at $x(\lambda_0)$ *homeostasis-bifurcation* points. We are interested in multiplicity and stability of solutions as well as homeostasis points in a particular Y variable, Y_k . In the case of steady-state bifurcation, we study homeostasis-bifurcation points by reducing the steady-state equation of (2),

$$F(Y, x) = 0, \quad (4)$$

to a scalar equation,

$$f(y, x) = 0 \quad (5)$$

that preserves the above properties. This can be done if we assume the nondegeneracy condition $e_k \notin (\ker(D_Y F)_{(Y_0, x_0)})^\perp$ where e_k is the unit vector in the k th direction (see Appendix A for details). In the case that (2) undergoes a Hopf bifurcation at (Y_0, x_0) , a reduction to (5) is still possible, but the nondegeneracy condition becomes $e_k \notin (\text{span}\{\text{Re}(v), \text{Im}(v)\})^\perp$ where v is an eigenvector of $(D_Y F)_{(Y_0, x_0)}$ whose eigenvalue is purely imaginary.

We define the codimension of a homeostasis-bifurcation point, $\text{codim}(x, f)$ or $\text{codim}(f(y, x(\lambda)))$ as the number of parameters needed in its unfolding. Intuitively,

$$\text{codim}(x, f) = \text{codim}_H(x) + \text{codim}_B(f) + 1 \quad (6)$$

as we need enough parameters to unfold $x(\lambda)$ and f individually and then an additional parameter to bring the two singularities together. This formula will be justified in Sec. 3.

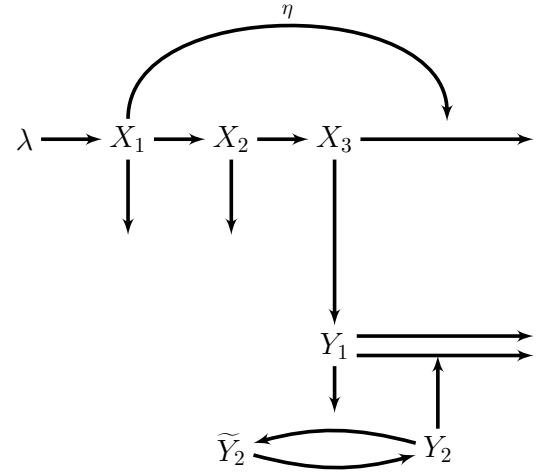


Fig. 1. A biochemical network exhibiting a chair-hysteresis point. X_3 has a chair point in λ and acts as the input to the Y system, which has a hysteresis point.

1.4. Homeostasis-bifurcation examples

Examples of biochemical networks with homeostasis-bifurcation points are given in Figs. 1 (homeostasis-steady-state bifurcation) and 2 (homeostasis-Hopf bifurcation). In each case the input-output function is $X_3(\lambda)$ and X_3 feeds into the Y network as its input. These networks are analyzed in detail in Sec. 2.

In the context of homeostasis, these points are interesting because the Y variables near these points tend to have more homeostatic properties than a homeostasis point alone would. In the case of steady-state bifurcation, the system may have multiple homeostatic plateaus and a natural way to switch between the plateaus as in Fig. 3. This type

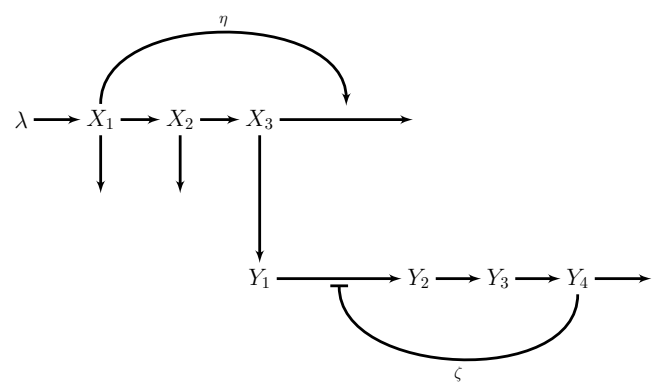


Fig. 2. A biochemical network exhibiting a chair-isola Hopf point. X_3 has a chair point in λ and acts as the input to the Y system, which has an isola-Hopf point.

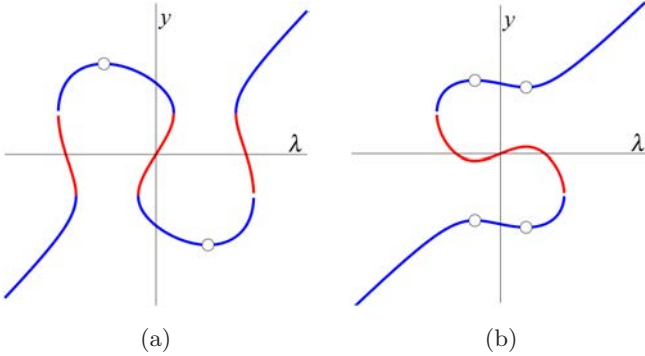


Fig. 3. Examples of multiple homeostatic plateaus in homeostasis-steady-state bifurcation. These diagrams arise from perturbations of the chair-hysteresis point. All perturbation types can be seen in Table 6 (item (6)). The blue (red) curves indicate stable (unstable) equilibria and homeostasis points are marked. These perturbations are particularly interesting because each has two homeostatic plateaus. In (a), the plateau that y lies in is predominantly determined by the current value of λ , while in (b) the choice of plateau is determined by the history of λ .

of behavior has been found in glycolysis [Mulukutla *et al.*, 2014] (see Fig. 4), for example. In the case of Hopf bifurcation, the amplitude and period of the limit cycles often have a wide range of near-constant

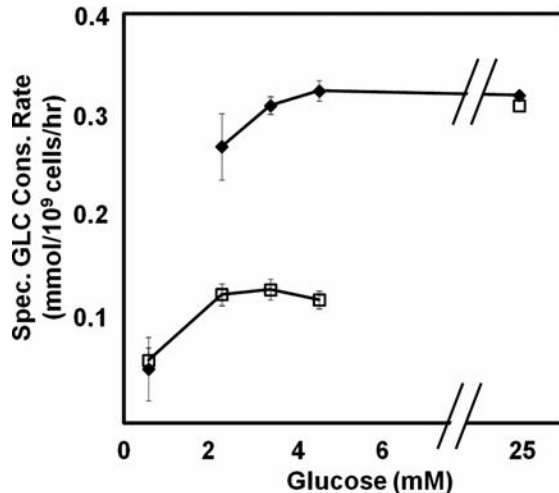


Fig. 4. Bistability in cultured HeLa cells (reproduced from [Mulukutla *et al.*, 2014]). Cells were initially cultured in high glucose (\blacklozenge) or low glucose (\square) and then resuspended in a medium with the indicated glucose concentration. The data suggests the existence of two homeostasis points on the lower branch: one which is apparent in the figure, and another which we would expect to see if it were extended further. The similar glucose consumption rates of both types of cells in very high and very low glucose environments indicate two switches on the border of the plateaus. The homeostasis points and the bistable behavior are suggestive of the behavior depicted in Fig. 3(a).

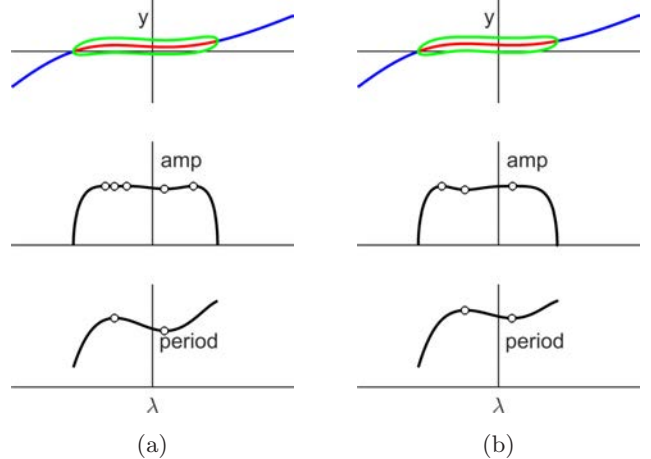


Fig. 5. Examples of homeostatic amplitude and period in homeostasis-Hopf bifurcation. These diagrams arise from perturbations of the chair-isola Hopf point. All perturbation types can be seen in Table 6 (item (11)⁺). The blue (red) curves indicate stable (unstable) equilibria. Green curves indicate the maxima and minima of stable limit cycles. Homeostasis points are marked.

amplitudes and periods as in Fig. 5. Circadian rhythms have been shown to maintain a period of about 24 h despite large changes in gene expression levels or variation in temperature [Dibner *et al.*, 2008; Bass & Takahashi, 2010]. Homeostasis-Hopf bifurcation is then a possible mechanism contributing to this phenomenon.

In the context of bifurcation, homeostasis-bifurcation points are interesting because the feed-forward structure restricts the space of allowable perturbations, therefore reducing the codimension. As a result, these points provide a way to access high codimension behavior through a low codimension singularity. For example, $\text{codim}_B(y^3 + \mu^3) = 5$, but $\text{codim}(\lambda^3, y^3 + \mu) = 3$. This is significant because low codimension phenomena are more common in applications.

1.5. Organization of this paper

In Sec. 2, we analyze the systems resulting from the networks in Figs. 1 and 2. In Sec. 3, we apply the unfolding theorems from elementary catastrophe theory and bifurcation theory to characterize the universal unfoldings of homeostasis-bifurcation points. In Sec. 4, we define the transition varieties and use standard singularity theory methods to prove that these are the only transitions that can occur. In Sec. 5, we use the theory developed in Secs. 3 and 4 to find the universal unfoldings and persistent phenomena for

the homeostasis-bifurcation points arising from the singularities in Tables 1 and 2. The paper ends with Appendix A describing the needed Lyapunov–Schmidt reduction in the context of combined homeostasis-bifurcation singularities.

2. Examples of Homeostasis–Bifurcation

In this section, we discuss two examples of homeostasis-bifurcation arising from the networks in Figs. 1 and 2. In each case we find a homeostasis-bifurcation point and all possible behaviors arising from perturbations away from this point. That these are in fact all possible behaviors is justified in Secs. 3–6.

Example 1. Chair-hysteresis in network of Fig. 1

Consider the network depicted in Fig. 1. The X network is the feedforward excitation network of [Reed *et al.*, 2017]. We assume mass action kinetics in the X component except for the degradation rate of X_3 , which is determined by the feedforward function, η . In the Y network, Y_1 catalyzes the reaction $Y_2 \rightarrow \tilde{Y}_2$ and Y_2 catalyzes the degradation of Y_1 . Y_1 is also degraded at a basal rate independent of Y_2 . We assume Michaelis–Menten kinetics in the reactions between Y_2 and \tilde{Y}_2 but mass action otherwise. Letting x_i and y_i denote the concentrations of X_i and Y_i , respectively, the differential

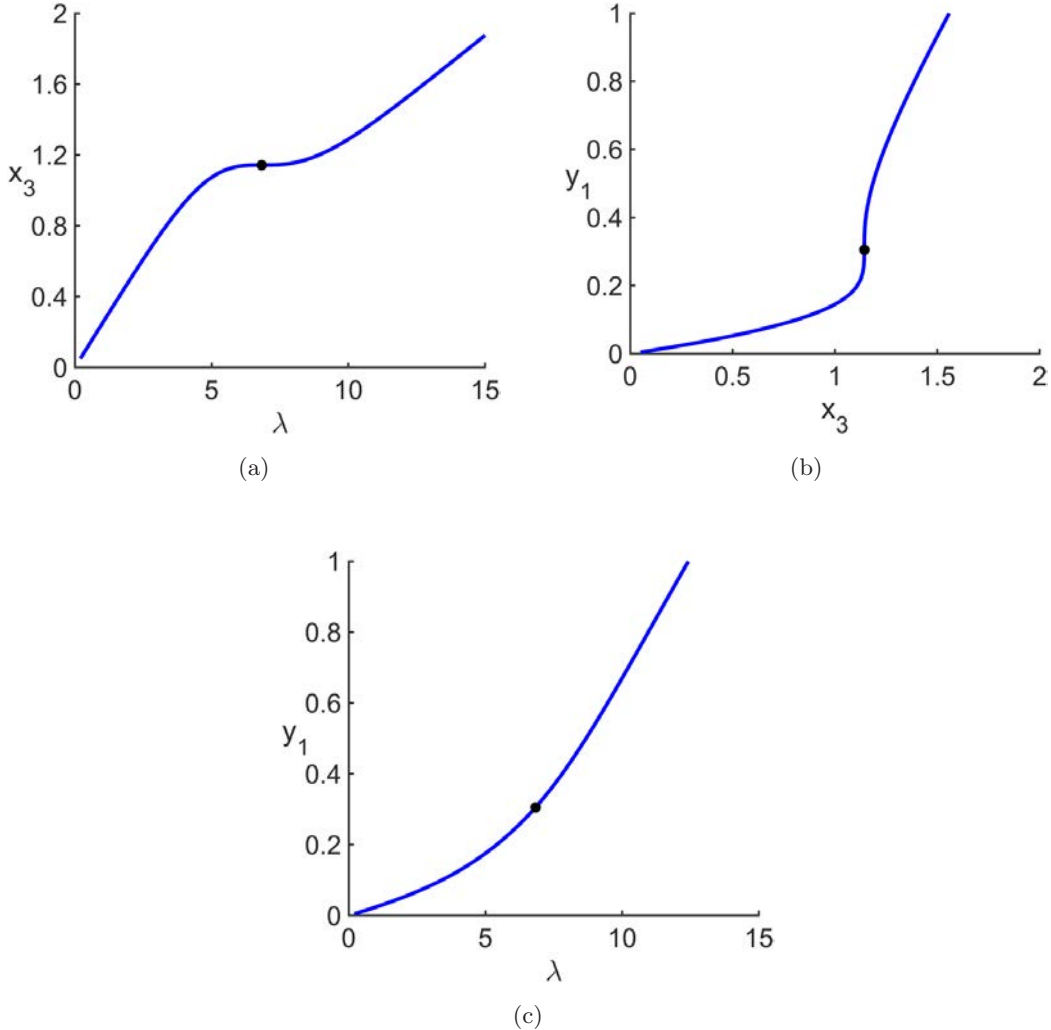


Fig. 6. The diagrams of x_3 and y_1 at the chair-hysteresis point. (a) The marked point indicates the chair point for $x_3(\lambda)$. (b) The marked point indicates the hysteresis point of the Y network with x_3 as the bifurcation parameter. (c) The chair-hysteresis point is marked. Neither homeostasis nor hysteresis are visible because the two singularities annihilate each other when they coincide.

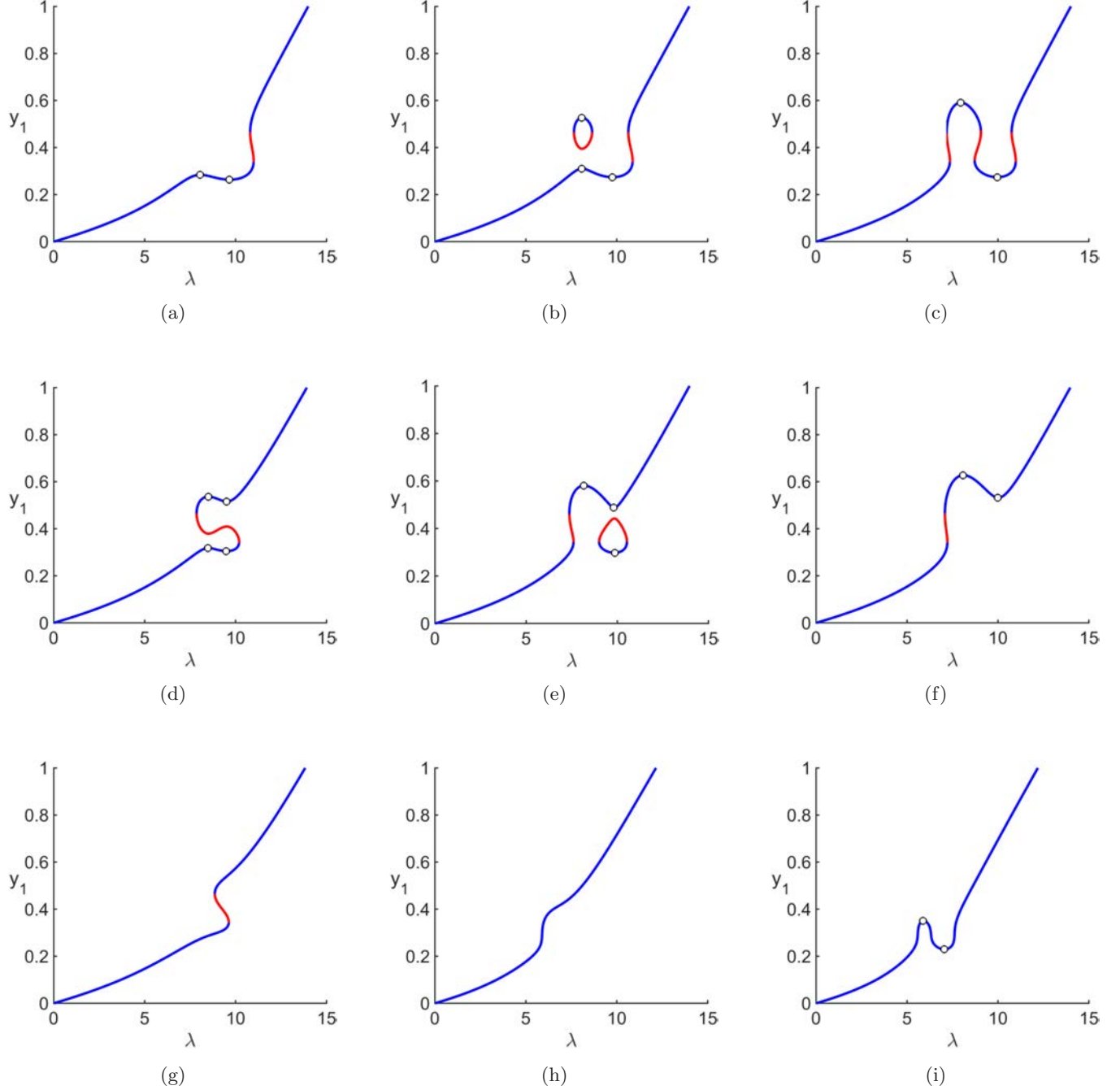


Fig. 7. Behavior of the chair-hysteresis network of Fig. 1. Each diagram corresponds to a persistent perturbation in Table 6 (item (6)). The blue (red) curves indicate stable (unstable) equilibria and homeostasis points are marked. The parameters chosen to construct each diagram are: (a) $a = 0.68, b = 12, c = 4.45$; (b) $a = 0.68, b = 12, c = 4.5$; (c) $a = 0.65, b = 12, c = 4.5$; (d) $a = 0.73, b = 12, c = 4.51$; (e) $a = 0.67, b = 12, c = 4.52$; (f) $a = 0.67, b = 12, c = 4.55$; (g) $a = 0.8, b = 12, c = 4.5$; (h) $a = 0.6, b = 18, c = 3.3$ and (i) $a = 0.5, b = 18, c = 3.25$.

equations for the network are given by

$$\begin{aligned}\dot{x}_1 &= \lambda - 2x_1, \\ \dot{x}_2 &= x_1 - 2x_2,\end{aligned}\tag{7}$$

$$\dot{x}_3 = x_2 - (1 + \eta(x_1))x_3,$$

$$\dot{y}_1 = x_3 - 2y_1y_2 - y_1,$$

$$\dot{y}_2 = -\frac{y_1y_2}{1+y_2} + \frac{\tilde{y}_2}{b+\tilde{y}_2},\tag{8}$$

$$\dot{\tilde{y}}_2 = \frac{y_1y_2}{1+y_2} - \frac{\tilde{y}_2}{b+\tilde{y}_2},$$

where $\eta(x) = \frac{1}{1+\gamma(x)}$ and $\gamma(x) = e^{\frac{c-x}{a}}$. λ is the input parameter while a, c , and b are auxiliary parameters. The output variable of the X network is x_3 . The steady-states also depend on the initial condition $y_2(0) + \tilde{y}_2(0)$, which we set to 5.

Repeating the analysis in [Reed *et al.*, 2017] shows that if $a = c/6$, then $x_3(\lambda)$ has a chair point at $\lambda_0 = 2c$ with $x_3(\lambda_0) = c/3$. For the Y network, if we treat x_3 as the bifurcation parameter, then we find a hysteresis point when $b = b^* \approx 16.91$ by using the numerical continuation software MatCont [Dhooge *et al.*, 2008]. Fix b at b^* , and let x_3^h be the value of x_3 at the hysteresis point. The network will have a chair-hysteresis point if $x_3(\lambda_0) = x_3^h$. Choosing $c = 3x_3^h$ therefore produces a chair-hysteresis point. Figure 6 shows $x_3(\lambda)$, the equilibria of y_1 as a function of x_3 , and the equilibria of y_1 as a function of λ at the chair-hysteresis point.

There are nine persistent perturbations of a chair-hysteresis point which are enumerated in Table 6 (item (6)). By choosing the parameters a, b , and c in (7) and (8) appropriately, we can reproduce all of these behaviors in the network (Fig. 7). The behaviors shown in Figs. 7(c) and 7(d) (and highlighted in Fig. 3) are of particular interest because each has two stable homeostatic plateaus corresponding to a low state and a high state. In the parameter region corresponding to Fig. 7(c), there are three hysteretic switches. The middle switch allows for switching between the two homeostatic plateaus while the outer switches define where the system escapes homeostasis. In the parameter region corresponding to Fig. 7(d), the low and high plateaus coexist over the same range of λ . In this case the state of the system would depend on the history of the input rather than its current value. This behavior could be desirable if it takes energy

to move λ outside of the plateau region, and without any external forcing, λ remains near the center of the plateau. The state of y_1 could then be controlled by bumping λ in the appropriate direction and then letting it relax back to center.

Example 2. Chair-isola Hopf in network of Fig. 2

Now consider the network depicted in Fig. 2. The X network is the same as above, and the Y network is adapted from [Duncan *et al.*, 2018]. We assume mass action kinetics for the Y network except for the reaction $Y_1 \rightarrow Y_2$, which is controlled by the feedback function ζ . The differential equations for the X network are given by (7), and the equations for the Y network are

$$\begin{aligned}\dot{y}_1 &= x_3 - \zeta(y_4)y_1, \\ \dot{y}_2 &= \zeta(y_4)y_1 - y_2, \\ \dot{y}_3 &= y_2 - y_3, \\ \dot{y}_4 &= y_3 - y_4,\end{aligned}\tag{9}$$

where we take $\zeta(y) = 10/(1+y^{10}) + b$. Using MatCont [Dhooge *et al.*, 2008], we find that there is an isola-Hopf bifurcation when $b = b^* \approx 0.011$. There are two simple Hopf bifurcations connected by a branch of stable limit cycles when $0 < b < b^*$ and there are no Hopf bifurcations when $b > b^*$.

As before, the input-output function is $x_3(\lambda)$. We take the distinguished Y variable to be y_4 . Letting x_3^H be the value of x_3 at the isola-Hopf bifurcation, there is a chair-isola Hopf point at $\lambda_0 = 2c$, if $c = 3x_3^H$ and $a = c/6$. Figure 8 shows the equilibrium values of y_4 at the singularity.

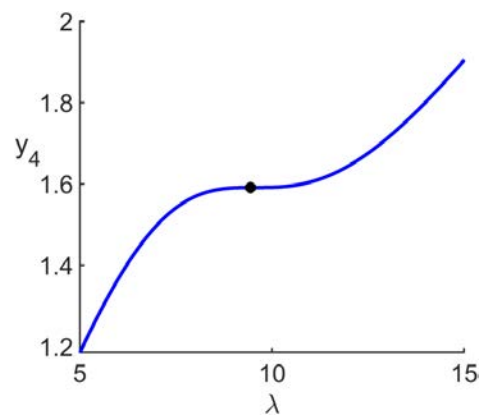


Fig. 8. Diagram of y_4 at the chair-isola Hopf point. The singularity is marked.

There are 13 persistent perturbations of the chair-isola Hopf which are enumerated in Table 6 (item (11)⁺). The corresponding diagrams for the network are shown in Fig. 9. The behaviors shown in Figs. 9(d), 9(f), 9(h) (and highlighted in Fig. 5)

are particularly interesting from the perspective of homeostasis. In Fig. 9(f), the limit cycle amplitudes are exceptionally homeostatic with five homeostasis points between the two Hopf bifurcations. In each of Figs. 9(d), 9(f), 9(h) the limit cycle periods are

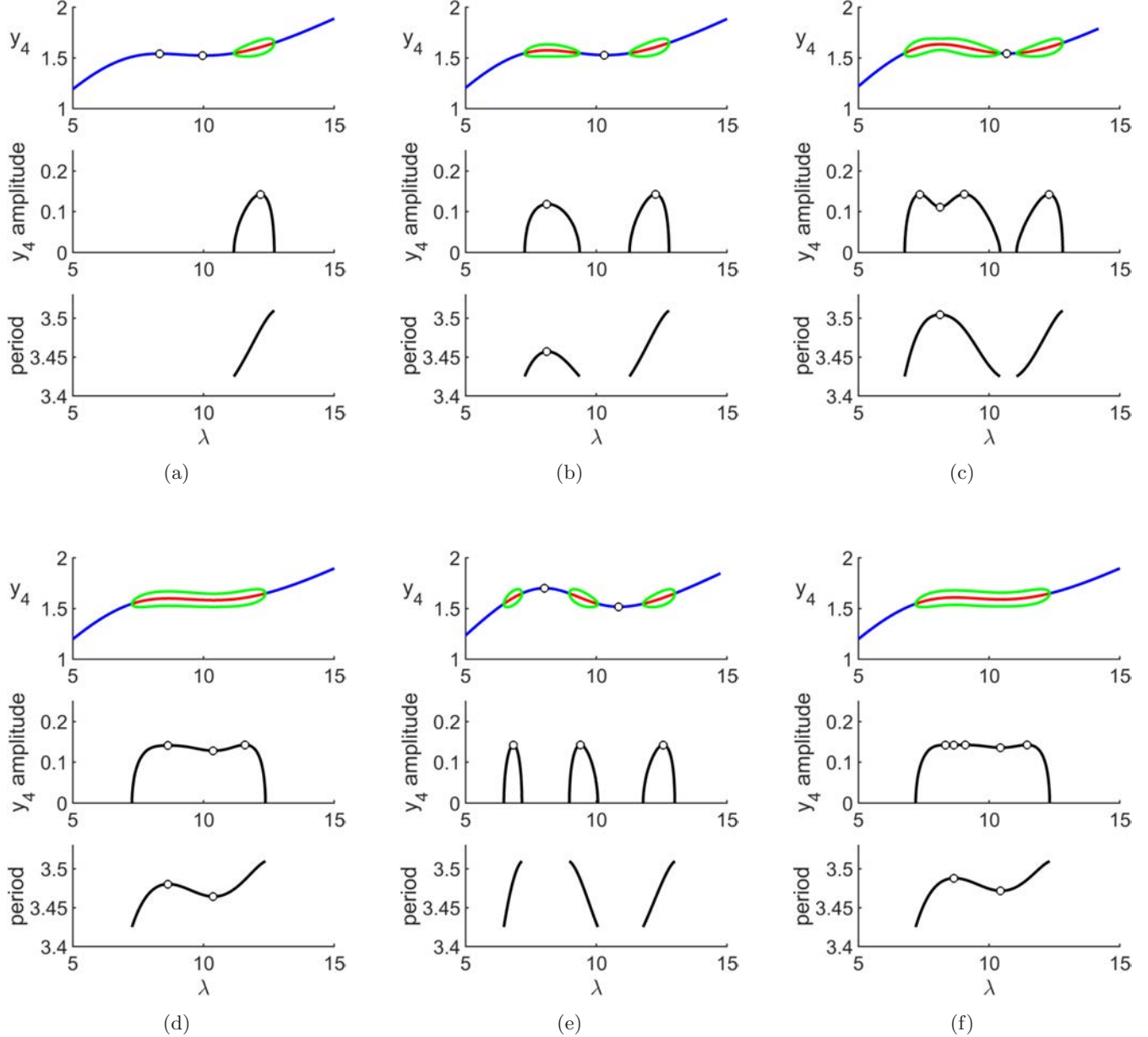


Fig. 9. Behavior of the chair-isola Hopf network in Fig. 2. Each diagram corresponds to a persistent perturbation in Table 6 (item (11)⁺). The blue (red) curves indicate stable (unstable) equilibria. The green curves indicate the maxima and minima of the stable limit cycles. The middle and bottom graphs show the amplitude and period of the limit cycles, respectively. Homeostasis points are marked. The parameters chosen to construct each diagram are: (a) $a = 0.7$, $b = 0.01$, $c = 4.6$; (b) $a = 0.65$, $b = 0.01$; (c) $a = 0.6$, $b = 0.01$, $c = 4.75$; (d) $a = 0.73$, $b = 0.01$, $c = 4.78$; (e) $a = 0.73$, $b = 0.01$, $c = 4.78$; (f) $a = 0.73$, $b = 0.01$, $c = 4.8$; (g) $a = 0.65$, $b = 0.01$, $c = 4.88$; (h) $a = 0.75$, $b = 0.01$, $c = 4.85$; (i) $a = 0.7$, $b = 0.01$, $c = 4.93$; (j) $a = 0.78$, $b = 0.01$, $c = 5$; (k) $a = 0.9$, $b = 0.01$, $c = 4.78$; (l) $a = 0.82$, $b = 0.11$, $c = 4.78$ and (m) $a = 0.7$, $b = 0.11$, $c = 4.78$.

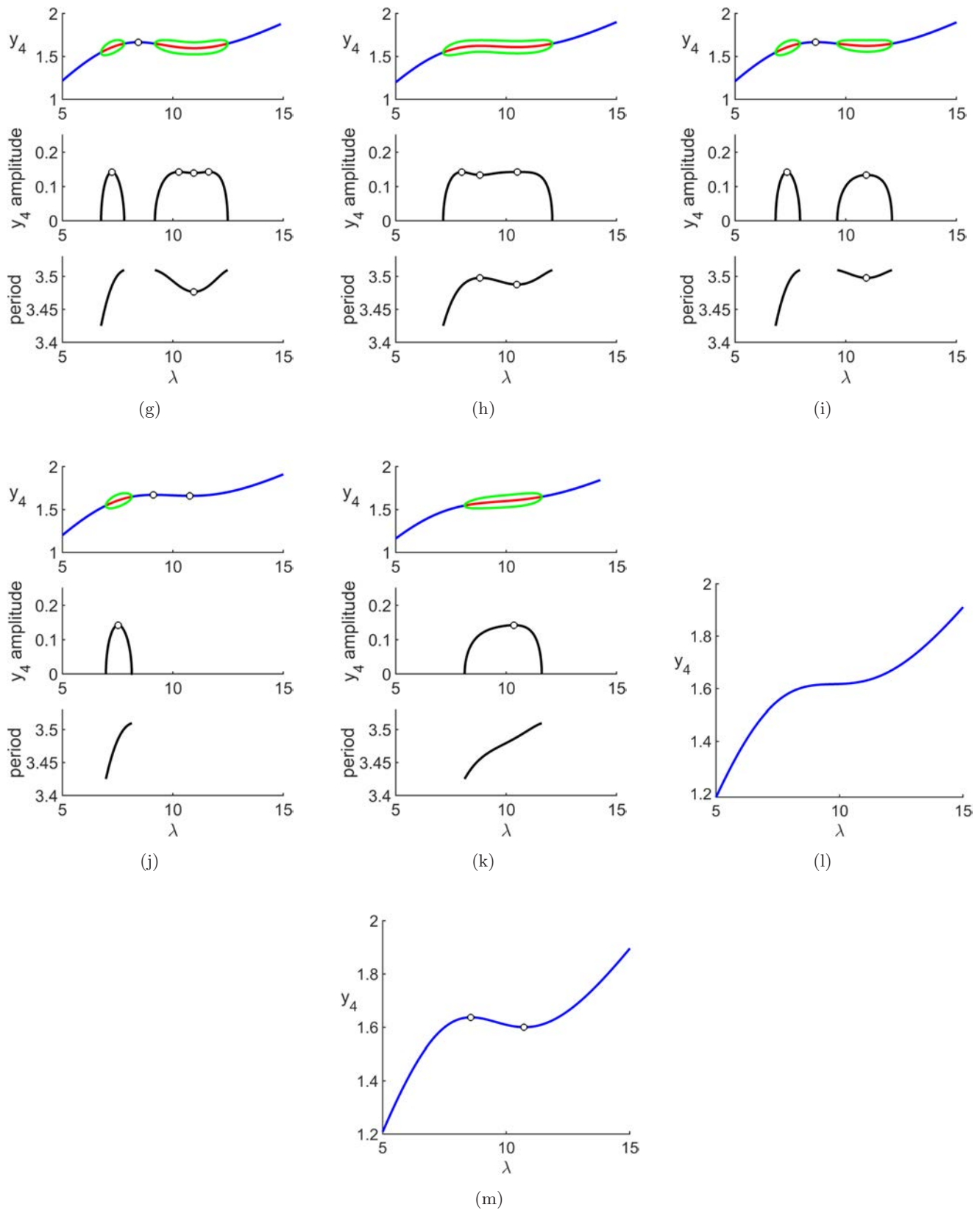


Fig. 9. (Continued)

homeostatic with two homeostasis points. Homeostatic period of limit cycles is desirable in biological clocks, for example.

3. Universal Unfoldings

In this section, we characterize the universal unfolding of homeostasis-bifurcation points. The allowable perturbations are those which respect the feed-forward structure of (1)–(2). That is, (1) and (2) can be independently perturbed, but the input–output function can never depend on the state variables of (2). For this reason, we can independently unfold the input–output function, x , and the bifurcation problem, f , and then link them together to obtain the unfolding of the homeostasis-bifurcation point, (x, f) .

First, we unfold the homeostasis point. Let $x(\lambda, a)$ be a family of input–output functions where λ is the input parameter and a parameterizes the family. $a \neq 0$ represents a perturbation away from the homeostasis point. Specifically, suppose x has a λ -homeostasis point at $(\lambda, a) = (0, 0)$ with $x(0, 0) = 0$. By the universal unfolding theorem in elementary catastrophe theory, $x(\lambda, a)$ factors through $\pm\lambda^k + a_{k-2}\lambda^{k-2} + \cdots + a_1\lambda$ where k is the first nonvanishing λ -derivative of x and $\text{codim}_H(x) = k - 2$ (see [Golubitsky & Stewart, 2016]). In particular we have

$$\begin{aligned} x(\lambda, a) = & \pm\Lambda(\lambda, a)^k + A_{k-2}(a)\Lambda(\lambda, a)^{k-2} \\ & + \cdots + A_1(a)\Lambda(\lambda, a) - C(a) \end{aligned} \quad (10)$$

where $\Lambda(0, 0) = 0$, $A(0) = 0$, $C(0) = 0$, and $\Lambda_\lambda > 0$.

Next, we unfold the bifurcation point. Let $f(y, \mu, b)$ be a family of functions with a bifurcation point at $(y, \mu, b) = (0, 0, 0)$. As before, b parameterizes the family and $b \neq 0$ indicates a perturbation from the bifurcation. Define $\ell := \text{codim}_B(f)$. By the universal unfolding theorem for bifurcations, $f(y, \mu, b)$ factors through a normal form, say $N(y, \mu, B)$ where $B \in \mathbb{R}^\ell$. That is,

$$f(y, \mu, b) = S(y, \mu, b)N(Y(y, \mu, b), M(\mu, b), B(b)) \quad (11)$$

where $S(0, 0, 0) > 0$, $Y(0, 0, 0) = 0$, $M(0, 0) = 0$, $B(0) = 0$, $Y_y(0, 0, 0) > 0$, and $M_\mu(0, 0) > 0$ (see [Golubitsky & Schaeffer, 1985]).

A homeostasis-bifurcation point is created by linking the input–output function, $x(\lambda)$, with the bifurcation problem, $f(y, \mu)$, to form $h(y, \lambda) := f(y, x(\lambda))$. Replacing x and f with their normal

form shows that h factors as

$$\begin{aligned} h(y, \lambda, a, b, c) = & S(x(\lambda, a), y, b)N(Y(x(\lambda, a), y, b), \\ & X(x(\lambda, a), b), B(b)). \end{aligned} \quad (12)$$

Therefore a universal unfolding for h is given by

$$N(y, \pm\lambda^k + a_{k-2}\lambda^{k-2} + \cdots + a_1\lambda - c, b). \quad (13)$$

Noting that there are $(k - 2) + \ell + 1 = \text{codim}_H(x) + \text{codim}_B(f) + 1$ parameters in this unfolding justifies formula (6).

4. Transition Varieties

In this section, we define the transition varieties of a homeostasis-bifurcation point. These are the set of points in parameter space across which the diagram qualitatively changes. Knowledge of these transition varieties allows us to find all possible behaviors near the homeostasis-bifurcation point.

Consider a perturbed version of (1)–(2):

$$\dot{X} = G(X, \lambda, a) \quad (14)$$

$$\dot{Y} = F(Y, x - c, b) \quad (15)$$

where we recall that $X \in \mathbb{R}^m$, $Y \in \mathbb{R}^n$, and $x = X_i$ is the distinguished, homeostatic variable of (14) and Y_k is the variable of interest. We assume (15) undergoes a steady-state or Hopf bifurcation at $(Y, x, b, c) = (0, 0, 0, 0)$. Let $x(\lambda, a)$ be the input–output function of (14) and $f(y, \mu, b)$ be an appropriate scalar reduction of (15) at the bifurcation point. Define $h(y, \lambda, a, b, c) = f(y, x(\lambda, a) - c, b)$. Let $U, L \subset \mathbb{R}$ be closed intervals and $(a, b, c) \in W \subset \mathbb{R}^\rho$. We take $U \times L \times W$ to be the domain of h . Solutions to $f = 0$ correspond to equilibria or amplitudes of limit cycles.

We will need the following definition from [Golubitsky & Schaeffer, 1985].

Definition 4.1. A branch of h is a continuous function $C : [L_1, L_2] \rightarrow U$ which is smooth on (L_1, L_2) and satisfies

- (1) $h(C(\lambda), \lambda) = 0$ on $[L_1, L_2]$, and
- (2) either $L_i \in \partial L$ or $(C(L_i), L_i)$ is a bifurcation point of h for $i = 1, 2$.

When (15) has a Hopf bifurcation, phase-shift symmetry forces f to be odd in y and that symmetry must be respected by perturbations. As a result, the transition varieties will differ depending on whether (15) has a steady-state or Hopf bifurcation. We first define the transition varieties for a steady-state bifurcation.

The transition varieties for homeostasis-steady-state bifurcation can be defined by conditions on h or by conditions on (x, f) . Defined by conditions on h they are as follows.

$$\mathcal{B} = \{(a, b, c) \mid \exists(y, \lambda) \text{ such that } h = h_\lambda = h_y = 0\},$$

$$\mathcal{H} = \{(a, b, c) \mid \exists(y, \lambda) \text{ such that } h = h_y = h_{yy} = 0\},$$

$$\mathcal{D} = \{(a, b, c) \mid \exists(y_1, y_2, \lambda) \text{ such that } h = h_y = 0$$

$$\text{at } (y_i, \lambda), i = 1, 2\},$$

$$\mathcal{C} = \{(a, b, c) \mid \exists(y, \lambda) \text{ such that } h = h_\lambda = h_{\lambda\lambda} = 0\}.$$

Note that \mathcal{B} , \mathcal{H} , and \mathcal{D} are the bifurcation, hysteresis, and double limit point transition varieties for h as a bifurcation point (see Chapter 3 of [Golubitsky & Schaeffer, 1985]). \mathcal{C} is the parameter set where a branch of h has a chair point.

In terms of x and f the transition varieties are

$$CH_x = \{(a, b, c) \mid \exists(x, y, \lambda)$$

$$\text{such that } \mu - x = f = x_\lambda = x_{\lambda\lambda} = 0\},$$

$$\mathcal{B} = \{(a, b, c) \mid \exists(x, y, \lambda)$$

$$\text{such that } \mu - x = f = f_\mu = f_y = 0\},$$

$$HYS = \{(a, b, c) \mid \exists(x, y, \lambda)$$

$$\text{such that } \mu - x = f = f_y = f_{yy} = 0\},$$

$$\mathcal{D} = \{(a, b, c) \mid \exists(x, \lambda, y_1, y_2), y_1 \neq y_2$$

$$\text{such that } \mu - x = f = f_y = 0$$

$$\text{at } (x, y_i, \lambda), i = 1, 2\},$$

$$CH_f = \{(a, b, c) \mid \exists(x, y, \lambda)$$

$$\text{such that } \mu - x = f = f_\mu = f_{\mu\mu} = 0\},$$

$$\mathcal{C} = \{(a, b, c) \mid \exists(x, y, \lambda)$$

$$\text{such that } \mu - x = f = f_y = x_\lambda = 0\},$$

$$HH = \{(a, b, c) \mid \exists(x, y, \lambda)$$

$$\text{such that } \mu - x = f = x_\lambda = f_\mu = 0\}.$$

CH_x is the set of parameters where x has a chair point. \mathcal{B} , HYS , and \mathcal{D} are the transition varieties of f as a bifurcation point. CH_f is where f has a branch with a chair point. \mathcal{C} and HH are due to interactions between x and f . \mathcal{C} is the coincidence transition variety consisting of points where homeostasis in x coincides with bifurcation in f . HH is where homeostasis in x coincides with homeostasis on a branch of f .

Proposition 1. *The two above definitions for the transition varieties are equivalent. That is, $CH_1 \cup \mathcal{B} \cup HYS \cup \mathcal{D} \cup \mathcal{C} \cup HH \cup CH_2 = \mathcal{B} \cup \mathcal{H} \cup \mathcal{D} \cup \mathcal{C}$.*

Proof. It is clear that $\mu - x(\lambda, a) = f(y, \mu - c, b) = 0$ if and only if $h(y, \lambda, a, b, c) = f(y, x(\lambda, a) - c, b) = 0$. Next, notice $h_\lambda = f_\mu x_\lambda$, $h_y = f_y$, $h_{yy} = f_{yy}$, and $h_{\lambda\lambda} = f_{\mu\mu} x_\lambda^2 + f_\mu x_{\lambda\lambda}$ so that we have

- (1) $h_\lambda = h_y = 0$ if and only if $(f_x = 0 \text{ or } x_\lambda = 0)$ and $f_y = 0$,
- (2) $h_y = h_{yy} = 0$ if and only if $f_y = f_{yy} = 0$,
- (3) $h_y = 0$ if and only if $f_y = 0$,
- (4) $h_\lambda = h_{\lambda\lambda} = 0$ if and only if $(x_\lambda = f_\mu = 0)$ or $(f_\mu = f_{\mu\mu} = 0)$ or $(x_\lambda = x_{\lambda\lambda} = 0)$.

Each of these, respectively, imply $\mathcal{B} = \mathcal{B} \cup \mathcal{C}$, $\mathcal{H} = HYS$, $\mathcal{D} = \mathcal{D}$, and $\mathcal{C} = HH \cup CH_2 \cup CH_1$. ■

In addition to these transition varieties, there are transitions which correspond to singularities occurring on the boundary of $U \times L$. For bifurcations, these are described in Chapter 4 of [Golubitsky & Schaeffer, 1985]. In the case of homeostasis-bifurcation, there are additional transitions corresponding to homeostasis points on the boundary. Dealing with these transitions is not difficult, but only serves to obscure the ideas, so we will assume that these boundary transitions do not occur.

Now suppose (15) undergoes a Hopf bifurcation at $(Y, x, b, c) = (0, 0, 0, 0)$. In this case we make an additional nondegeneracy assumption. We may apply the implicit function theorem to $F(Y, x, 0) = 0$ to obtain a curve of equilibria, $Y(x)$. We assume $Y'(x) \neq 0$. This assumption guarantees that locally the only equilibrium homeostasis points of Y_k are inherited by x . The reduction of (15) yields $f(y, \mu, b) = \rho(y^2, \mu, b)y$ for some function $\rho(u, \mu, b)$. Define $r(u, \lambda, a, b, c) = \rho(u, x(\lambda, a) - c, b)$. h is then given by $h(y, \lambda, a, b, c) = r(y^2, \lambda, a, b, c)y$. The transition varieties can be defined by conditions on r and x only. They are as follows.

$$\mathcal{B}_H = \{(a, b, c) \mid \exists(u, \lambda), u > 0 \text{ such that}$$

$$r = r_\lambda = r_u = 0\},$$

$$\mathcal{B}_0 = \{(a, b, c) \mid \exists \lambda \text{ such that at } u = 0,$$

$$r = r_\lambda = 0\},$$

$$\mathcal{H}_H = \{(a, b, c) \mid \exists(u, \lambda), u > 0 \text{ such that}$$

$$r = r_u = r_{uu} = 0\},$$

$$\mathcal{H}_0 = \{(a, b, c) \mid \exists \lambda \text{ such that at } u = 0,$$

$$r = r_u = 0\},$$

$$\mathcal{D}_H = \{(a, b, c) \mid \exists (u_1, u_2, \lambda) u \geq 0 \text{ such that}$$

$$r = r_u = 0 \text{ at } (u_i, \lambda), i = 1, 2\},$$

$$\mathcal{C}_H = \{(a, b, c) \mid \exists (u, \lambda), u > 0 \text{ such that}$$

$$r = r_\lambda = r_{\lambda\lambda} = 0\},$$

$$CH_H = \{(a, b, c) \mid \exists \lambda \text{ such that } x_\lambda = x_{\lambda\lambda} = 0\}.$$

These are the standard transition varieties for h treated as a bifurcation with the addition of \mathcal{C}_H , which accounts for chair points of the amplitude, and CH_H which accounts for chair points on the equilibria.

We use the definition involving h for the steady-state transitions in what follows. Define

$$\Sigma = \mathcal{B} \cup \mathcal{H} \cup \mathcal{D} \cup \mathcal{C} \quad \text{or}$$

$$\Sigma = \mathcal{B}_H \cup \mathcal{B}_0 \cup \mathcal{H}_H \cup \mathcal{H}_0 \cup \mathcal{D}_H \cup \mathcal{C}_H \cup CH_H$$

as appropriate. To simplify notation, collect the parameters into a single variable $\alpha = (a, b, c) \in W$. We will show that if (15), $\alpha, \beta \in W \setminus \Sigma$ are in the same connected component of $W \setminus \Sigma$, then $h(y, \lambda, \alpha)$ and $h(y, \lambda, \beta)$ have the same diagram. Because Σ is a superset of the bifurcation transition varieties, we immediately have

Proposition 2. *Let α and β be in the same connected component of $W \setminus \Sigma$ and suppose there are no boundary transitions. Then $h(\cdot, \cdot, \alpha)$ and $h(\cdot, \cdot, \beta)$ are equivalent as bifurcation problems.*

Proof. See Theorem 10.1 in Chapter 3 and Theorem 4.1 in Chapter 6 of [Golubitsky & Schaeffer, 1985]. ■

Equivalence as bifurcations means $h(\cdot, \cdot, \alpha)$ and $h(\cdot, \cdot, \beta)$ have the same bifurcation diagram. In particular, it allows us to identify branches of $h(\cdot, \cdot, \alpha)$ and $h(\cdot, \cdot, \beta)$ with each other. This identification allows us to determine if the branches have the same number of homeostasis points.

Theorem 1. *Let α and β be in the same connected component of $W \setminus \Sigma$ and suppose that there are no boundary transitions. Then if C^α and C^β are corresponding branches of $h(\cdot, \cdot, \alpha)$ and $h(\cdot, \cdot, \beta)$ with homeostasis points $\nu_1 < \nu_2 < \dots < \nu_i$ and $\sigma_1 < \sigma_2 < \dots < \sigma_j$ respectively, then $i = j$ and $\text{sign}(C^\alpha''(\nu_m)) = \text{sign}(C^\beta''(\sigma_m))$ for each m .*

Proof. Differentiating $h(C^\alpha(\lambda), \lambda, \alpha)$ in λ and using $\alpha \notin \mathcal{C}$ or $\alpha \notin \mathcal{C}_H$ shows that C^α' and C^α'' cannot simultaneously vanish. The same statement is true for C^β . This fact and the compactness of the domains of C^α and C^β together imply that there are only a finite number of homeostasis points on each branch. Therefore, the enumeration in the statement of the theorem is well defined.

Let $\alpha(t)$ be a path in a connected component of $W \setminus \Sigma$ with $\alpha(0) = \alpha$ and $\alpha(1) = \beta$. For each $t \in [0, 1]$, we can identify a branch of $h(\cdot, \cdot, \alpha(t))$ with C^α because the reduced functions are equivalent as bifurcations by Proposition 2. Name this branch C^t . Note that $C^0 = C^\alpha$ and $C^1 = C^\beta$.

Let $t_0 \in [0, 1]$ and $\lambda_1 < \lambda_2 < \dots < \lambda_\ell$ be the set of points where $\phi(\lambda, t_0) := C^{t_0}'(\lambda)$ vanishes. For each i , $\phi(\lambda_i, t_0) = 0$ and $\phi_\lambda(\lambda_i, t_0) = C^{t_0}''(\lambda_i) \neq 0$. So, by the implicit function theorem, there is a smooth curve, $\Lambda_i(t)$ so that $\phi(\Lambda_i(t), t) = 0$ for t near t_0 . We can construct such a function for any $t_0 \in [0, 1]$. By the compactness of $[0, 1]$ we can patch together these curves and define $\Lambda_i(t)$ globally on $[0, 1]$. Uniqueness, implied by the implicit function theorem, then guarantees that $\ell = i = j$ and the ordering is preserved as the curves cannot cross.

For each t , $C^{t'}(\Lambda_i(t)) = 0$ and $C^{t''}(\Lambda_i(t)) \neq 0$. So by continuity, $\text{sign}(C_k^{t''}(\Lambda_i(t)))$ is constant and in particular $\text{sign}(C^\alpha''(\nu_i)) = \text{sign}(C^\beta''(\sigma_i))$. ■

Proposition 2 and Theorem 1 together imply that the diagrams of h are qualitatively the same on connected components of $W \setminus \Sigma$ in the case of steady-state bifurcation. For Hopf bifurcation, this does not rule out homeostasis transitions for the equilibria solutions. Our assumption that the equilibria $Y'_k(x) \neq 0$ at the Hopf bifurcation means homeostasis in $Y_k(x(\lambda))$ can only be inherited from x . CH_H thus accounts for these transitions. It is possible that (14)–(15) have the same diagram on different connected components. Indeed Sec. 5 contains examples of this.

5. Low Codimension Homeostasis-Bifurcation Points

In this section, we provide all information for the homeostasis-bifurcation points arising from the singularities in Tables 1 and 2. The information is organized into Tables 3–6 with the numbers in parentheses indicating how to link the information between tables. When plotting the diagrams of persistent

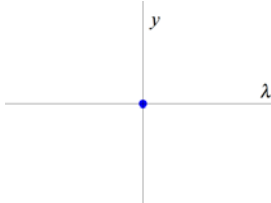
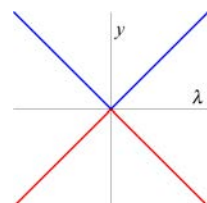
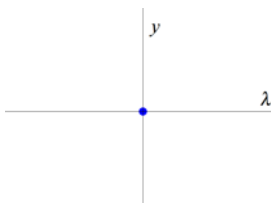
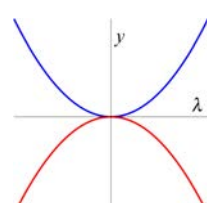
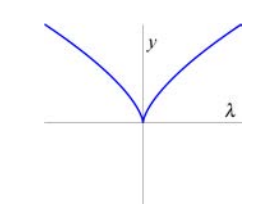
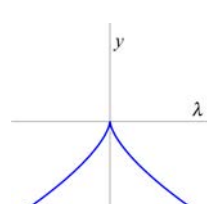
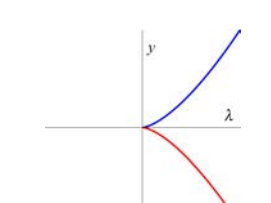
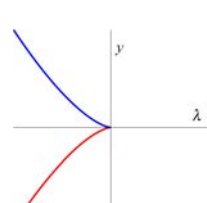
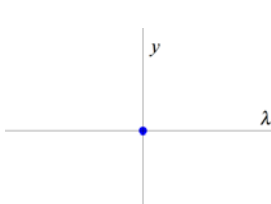
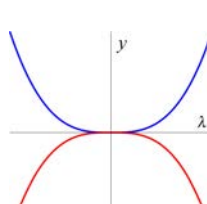
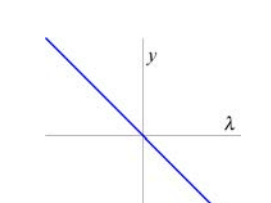
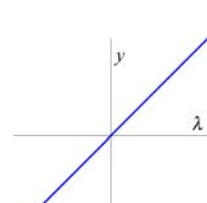
Table 3. Defining conditions.

	Normal Form	Defining Conditions*	Nondegeneracy Conditions
Homeostasis-steady-state bifurcations			
(1)	$x(\lambda) = \eta\lambda^2$ $f(y, \mu) = \varepsilon y^2 + \delta\mu$		$\eta = \text{sign}(x_{\lambda\lambda})$ $\varepsilon = \text{sign}(f_{yy}), \quad \delta = \text{sign}(f_\mu)$
(2)	$x(\lambda) = \eta\lambda^2$ $f(y, \mu) = \varepsilon(y^2 + \delta\mu^2)$	$f_\mu = 0$	$\eta = \text{sign}(x_{\lambda\lambda})$ $\varepsilon = \text{sign}(f_{yy}), \quad \delta = \text{sign}(\det d^2 f)$
(3)	$x(\lambda) = \eta\lambda^2$ $f(y, \mu) = \varepsilon y^3 + \delta\mu$	$f_{yy} = 0$	$\eta = \text{sign}(x_{\lambda\lambda})$ $\varepsilon = \text{sign}(f_{yyy}), \quad \delta = \text{sign}(f_\mu)$
(4)	$x(\lambda) = \eta\lambda^3$ $f(y, \mu) = \varepsilon y^2 + \delta\mu$	$x_{\lambda\lambda} = 0$	$\eta = \text{sign}(x_{\lambda\lambda\lambda})$ $\varepsilon = \text{sign}(f_{yy}), \quad \delta = \text{sign}(f_\mu)$
(5)	$x(\lambda) = \eta\lambda^3$ $f(y, \mu) = \varepsilon(y^2 + \delta\mu^2)$	$x_{\lambda\lambda} = 0$ $f_\mu = 0$	$\eta = \text{sign}(x_{\lambda\lambda\lambda})$ $\varepsilon = \text{sign}(f_{yy}), \quad \delta = \text{sign}(\det d^2 f)$
(6)	$x(\lambda) = \eta\lambda^3$ $f(y, \mu) = \varepsilon y^3 + \delta\mu$	$x_{\lambda\lambda} = 0$ $f_{yy} = 0$	$\eta = \text{sign}(x_{\lambda\lambda\lambda})$ $\varepsilon = \text{sign}(f_{yy}), \quad \delta = \text{sign}(f_\mu)$
Homeostasis-Hopf bifurcations			
(7)	$x(\lambda) = \eta\lambda^2$ $f(y, \mu) = (\varepsilon y^2 + \delta\mu)y$		$\eta = \text{sign}(x_{\lambda\lambda})$ $\varepsilon = \text{sign}(\rho_u), \quad \delta = \text{sign}(\rho_\mu)$
(8)	$x(\lambda) = \eta\lambda^2$ $f(y, \mu) = (\varepsilon y^2 + \delta\mu^2)y$	$\rho_\mu = 0$	$\eta = \text{sign}(x_{\lambda\lambda})$ $\varepsilon = \text{sign}(\rho_u), \quad \delta = \text{sign}(\rho_{\mu\mu})$
(9)	$x(\lambda) = \eta\lambda^2$ $f(y, \mu) = (\varepsilon y^4 + \delta\mu)y$	$\rho_u = 0$	$\eta = \text{sign}(x_{\lambda\lambda})$ $\varepsilon = \text{sign}(\rho_{uu}), \quad \delta = \text{sign}(\rho_\mu)$
(10)	$x(\lambda) = \eta\lambda^3$ $f(y, \mu) = (\varepsilon y^2 + \delta\mu)y$	$x_{\lambda\lambda} = 0$	$\eta = \text{sign}(x_{\lambda\lambda\lambda})$ $\varepsilon = \text{sign}(\rho_u), \quad \delta = \text{sign}(\rho_\mu)$
(11)	$x(\lambda) = \eta\lambda^2$ $f(y, \mu) = (\varepsilon y^2 + \delta\mu^2)y$	$x_{\lambda\lambda} = 0$ $\rho_\mu = 0$	$\eta = \text{sign}(x_{\lambda\lambda\lambda})$ $\varepsilon = \text{sign}(\rho_u), \quad \delta = \text{sign}(\rho_{\mu\mu})$
(12)	$x(\lambda) = \eta\lambda^2$ $f(y, \mu) = (\varepsilon y^4 + \delta\mu)y$	$x_{\lambda\lambda} = 0$ $\rho_u = 0$	$\eta = \text{sign}(x_{\lambda\lambda\lambda})$ $\varepsilon = \text{sign}(\rho_{uu}), \quad \delta = \text{sign}(\rho_\mu)$

For Hopf bifurcations, $\rho(u, \mu)$ is defined by $f(y, \mu) = \rho(y^2, \mu)y$. The numbers link information between tables.

*We always assume $x_\lambda = 0$ and $f = f_y = 0$. For Hopf bifurcations, we assume $\rho = 0$.

Table 4. Universal unfoldings.

Universal Unfolding	Unperturbed Diagrams ($\varepsilon = -1, \eta = 1$)	
	$\delta = 1$	$\delta = -1$
(1) $x(\lambda) = \eta\lambda^2$ $f(y, \mu, c) = \varepsilon y^2 + \delta(\mu - c)$		
(2) $x(\lambda) = \eta\lambda^2$ $f(y, \mu, c) = \varepsilon(y^2 + \delta(\mu - c)^2 + b)$		
(3) $x(\lambda) = \eta\lambda^2$ $f(y, \mu, c) = \varepsilon y^3 + \delta(\mu - c) + by$		
(4) $x(\lambda) = \eta\lambda^3 + a\lambda$ $f(y, \mu, c) = \varepsilon y^2 + \delta(\mu - c)$		
(5) $x(\lambda) = \eta\lambda^3 + a\lambda$ $f(y, \mu, c) = \varepsilon(y^2 + \delta(\mu - c)^2 + b)$		
(6) $x(\lambda) = \eta\lambda^3 + a\lambda$ $f(y, \mu, c) = \varepsilon y^3 + \delta(\mu - c) + by$		

Blue (red) curves indicate stable (unstable) equilibria. Black curves indicate amplitudes of stable limit cycles. The numbers link information between tables.

Table 4. (Continued)

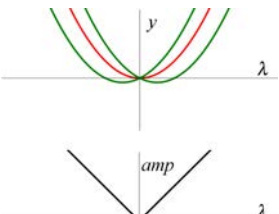
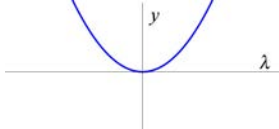
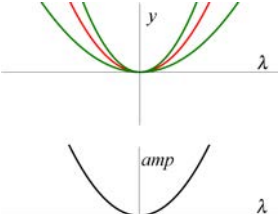
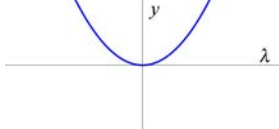
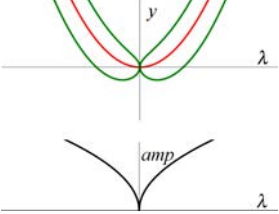
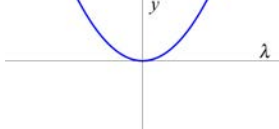
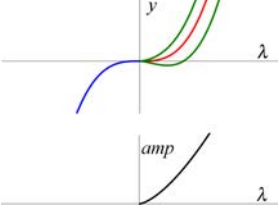
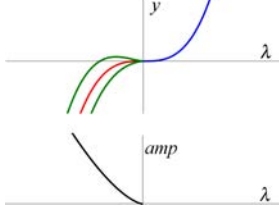
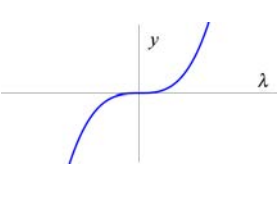
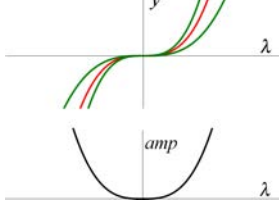
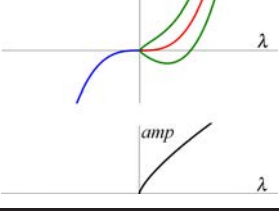
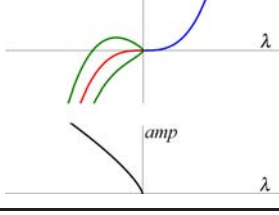
Universal Unfolding	Unperturbed Diagrams ($\varepsilon = -1, \eta = 1$)	
	$\delta = 1$	$\delta = -1$
(7) $x(\lambda) = \eta\lambda^2$ $f(y, \mu, c) = \varepsilon y^3 + \delta(\mu - c)y$		
(8) $x(\lambda) = \eta\lambda^2$ $f(y, \mu, c) = \varepsilon y^3 + \delta(\mu - c)^2y + by$		
(9) $x(\lambda) = \eta\lambda^2$ $f(y, \mu, c) = \varepsilon y^5 + \delta(\mu - c)y + by^3$		
(10) $x(\lambda) = \eta\lambda^3 + a\lambda$ $f(y, \mu, c) = \varepsilon y^3 + \delta(\mu - c)y$		
(11) $x(\lambda) = \eta\lambda^3 + a\lambda$ $f(y, \mu, c) = \varepsilon y^3 + \delta(\mu - c)^2y + by$		
(12) $x(\lambda) = \eta\lambda^3 + a\lambda$ $f(y, \mu, c) = \varepsilon y^5 + \delta(\mu - c)y + by^3$		

Table 5. Transition varieties.

	Normal Form, h	\mathcal{B}	\mathcal{H}	\mathcal{C}
(1) +	$-y^2 + \lambda^2 - c$	$\{c = 0\}$	\emptyset	\emptyset
(1) -	$-y^2 - \lambda^2 + c$	$\{c = 0\}$	\emptyset	\emptyset
(2) +	$-y^2 - (\lambda^2 - c)^2 + b$	$\{b = 0 \mid c \geq 0\} \cup \{b = c^2\}$	\emptyset	$\{c = 0 \mid b \geq 0\}$
(2) -	$-y^2 + (\lambda^2 - c)^2 + b$	$\{b = 0 \mid c \geq 0\} \cup \{b = -c^2\}$	\emptyset	$\{c = 0 \mid b \geq 0\}$
(3)	$-y^3 + \lambda^2 - c + by$	$\left\{ -\theta \left(\frac{b}{3} \right)^{\frac{3}{2}} + \theta b \left(\frac{b}{3} \right)^{\frac{1}{2}} = c \right\}$	$\{b = 0 \mid c \geq 0\}$	\emptyset
(4)	$-y^2 + \lambda^3 + a\lambda - c$	$\left\{ 2\theta \left(\frac{-a}{3} \right)^{\frac{3}{2}} = c \mid a \leq 0 \right\}$	\emptyset	$\{a = 0 \mid c \leq 0\}$
(5) +	$-y^2 + (\lambda^3 + a\lambda - c)^2 + b$	$\left\{ - \left(2\theta \left(\frac{-a}{3} \right)^{\frac{3}{2}} - c \right)^2 = b \mid a \leq 0 \right\} \cup \{b = 0\}$	\emptyset	$\left\{ 2\theta \left(\frac{-a}{3} \right)^{\frac{3}{2}} = c \mid a \leq 0, b \leq 0 \right\} \cup \{a = 0 \mid c^2 = -b\}$
(5) -	$-y^2 - (\lambda^3 + a\lambda - c)^2 + b$	$\left\{ \left(2\theta \left(\frac{-a}{3} \right)^{\frac{3}{2}} - c \right)^2 = ba \leq 0 \right\} \cup \{b = 0\}$	\emptyset	$\left\{ 2\theta \left(\frac{-a}{3} \right)^{\frac{3}{2}} = c \mid a \leq 0, b \leq 0 \right\} \cup \{a = 0 \mid c^2 \geq b\}$
(6)	$-y^3 + \lambda^+ a\lambda - c + by$	$\left\{ \theta_1 \left(\frac{-a}{3} \right)^{\frac{3}{2}} + \theta_2 \left(\frac{b}{3} \right)^{\frac{3}{2}} = 0 \mid a \leq 0, b \geq 0 \right\}$	$\{b = 0\}$	$\{a = 0\}$

where $\theta = 1$ or -1 . $\mathcal{D} = \emptyset$ for each homeostasis-bifurcation point considered here. As in Table 4 we choose $\varepsilon = -1$ and $\eta = 1$. The numbers link information between tables with (+) or (-) indicating the sign of δ where appropriate. $\delta = 1$ otherwise.

Table 5. (Continued)

	Normal Form, h	\mathcal{B}	\mathcal{H}	\mathcal{C}
(7) ⁺	$-y^3 + (\lambda^2 - c)y$	$\{c = 0\}$	\emptyset	\emptyset
(7) ⁻	$-y^3 - (\lambda^2 - c)y$	$\{c = 0\}$	\emptyset	\emptyset
(8) ⁺	$-y^3 + (\lambda^2 - c)^2 y + by$	$\{b = 0 \mid c \geq 0\} \cup \{c^2 = -b\}$	\emptyset	$\{c = 0 \mid b \geq 0\}$
(8) ⁻	$-y^3 - (\lambda^2 - c)^2 y + by$	$\{b = 0 \mid c \geq 0\} \cup \{c^2 = -b\}$	\emptyset	$\{c = 0 \mid b \leq 0\}$
(9) ⁺	$-y^5 + (\lambda^2 - c)y + by^3$	$\left\{ \frac{b^2}{4} = c \right\} \cup \{c = 0\}$	$\{b = 0 \mid c \geq 0\}$	\emptyset
(9) ⁻	$-y^5 - (\lambda^2 - c)y + by^3$	$\left\{ \frac{b^2}{4} = -c \right\} \cup \{c = 0\}$	$\{b = 0 \mid c \leq 0\}$	\emptyset
(10)	$-y^3 + (\lambda^3 + a\lambda - c)y$	$\left\{ 2\theta\left(\frac{-a}{3}\right)^{\frac{3}{2}} = c \mid a \leq 0 \right\}$	\emptyset	$\{a = 0\}$
(11)	$-y^3 + (\lambda^3 + a\lambda - c)^2 y + by$	$\left\{ \left(2\theta\left(\frac{-a}{3}\right)^{\frac{3}{2}} - c \right)^2 = b \mid a \leq 0 \right\} \cup \{b = 0\}$	\emptyset	$\left\{ 2\theta\left(\frac{-a}{3}\right)^{\frac{3}{2}} = c \mid a \leq 0, b \leq 0 \right\} \cup \{a = 0\}$
(12)	$-y^5 + (\lambda^3 + a\lambda - c)y + by^3$	$\left\{ (2^{\frac{2}{3}} - 1) \left(\frac{b}{2}\right)^{\frac{4}{3}} + 2\theta\left(\frac{-a}{3}\right)^{\frac{3}{2}} = c \mid a \leq 0, b \geq 0 \right\}$	$\{b = 0\}$	$\{a = 0\}$
		$\cup \left\{ 2\theta\left(\frac{-a}{3}\right)^{\frac{3}{2}} = c \mid a \leq 0 \right\}$		

Table 6. Persistent diagrams.

Transition Variety Σ	Persistent Perturbations
(1) ⁺ Simple homeostasis — limit point: $-y^2 + \lambda^2 - c$	 (a) (b) No solutions
(1) ⁻ Simple homeostasis — limit point: $-y^2 - \lambda^2 + c$	 (a) (b)
(2) ⁺ Simple homeostasis — isolas: $-y^2 - (\lambda^2 - c)^2 + b$	 No solutions
(2) ⁻ Simple homeostasis — simple bifurcation: $-y^2 + (\lambda^2 - c)^2 + b$	

Blue (red) curves indicate stable (unstable) equilibria. Homeostasis points are marked. Region (2)⁺(c) has a homeostatic plateau for which leaving the plateau is marked by a loss of steady-state. Region (2)⁻(d) predicts a wide homeostatic plateau.

Table 6. (Continued)

Transition Variety Σ	Persistent Perturbations
(3) Simple homeostasis — hysteresis: $-y^3 + \lambda^2 - c + by$	
(4) Chair — limit point: $-y^2 + \lambda^3 + a\lambda - c$	
(5) ⁺ Chair — isola: $-y^2 - (\lambda^3 + a\lambda - c)^2 - b$	<p style="text-align: center;">$b < 0$</p> <p style="text-align: center;">No solutions when $b > 0$</p>

Blue (red) curves indicate stable (unstable) equilibria. Homeostasis points are marked. (5)⁺ has many regions which predict wide plateaus for which leaving the plateau is marked by a loss of steady-state. Region (5)⁺(e) is exceptionally homeostatic.

Table 6. (Continued)

Transition Variety Σ	Persistent Perturbations		
	(g)	(h)	(i)
(5) ⁻ Chair — simple bifurcation: $-y^2 + (\lambda^3 + a\lambda - c)^2 - b$			

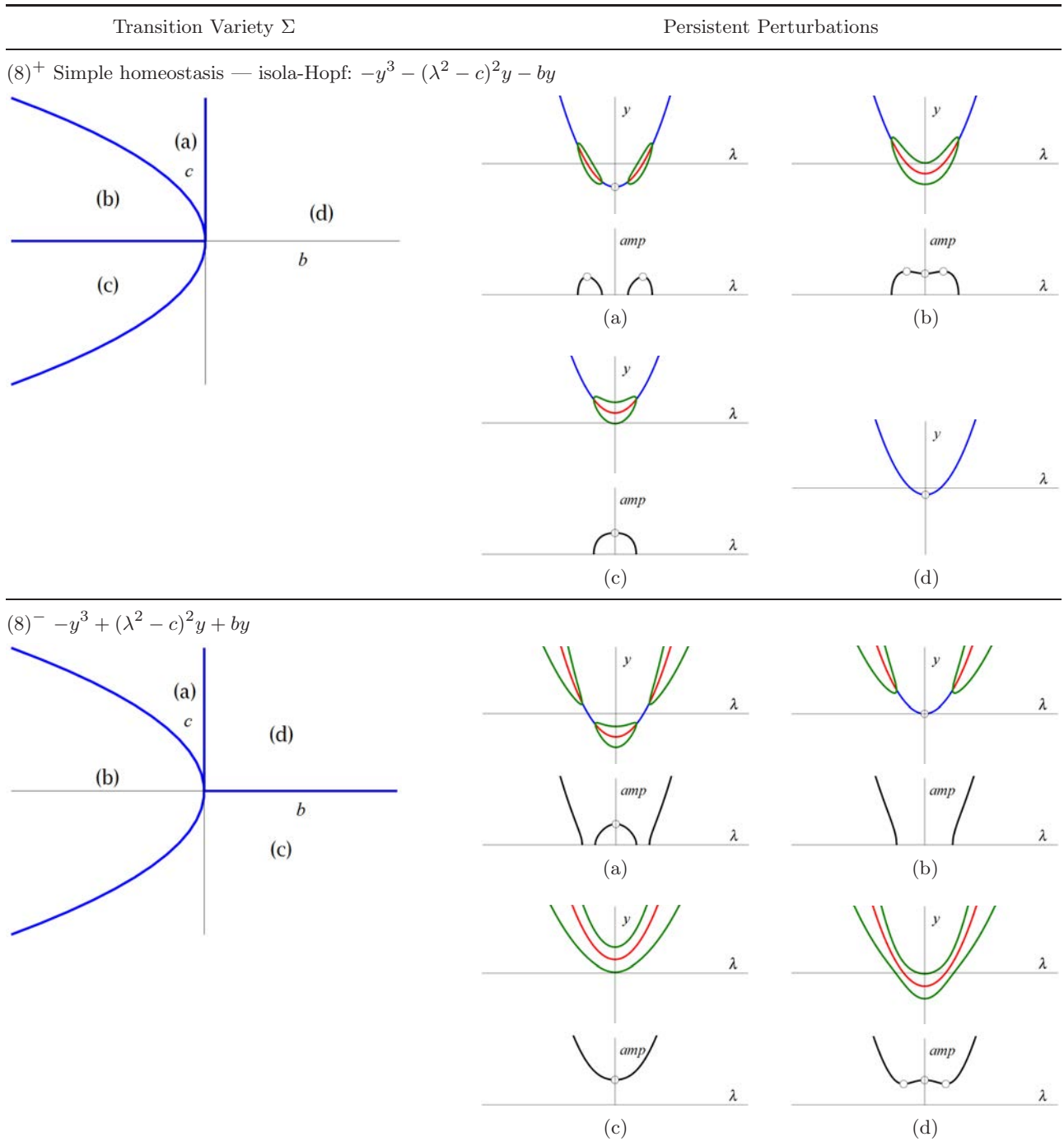
Blue (red) curves indicate stable (unstable) equilibria. Homeostasis points are marked. Region (5)⁻(b) predicts a particularly wide plateau. Regions (5)⁻(e) and (5)⁻(i) predict a plateau for which variation in one direction is marked by loss of steady-state.

Table 6. (Continued)

Transition Variety Σ	Persistent Perturbations		
(6) Chair — hysteresis: $-y^3 + \lambda^3 + a\lambda - c + by$			
(7) ⁺ Simple homeostasis — simple Hopf: $-y^3 - (\lambda^2 - c)y$			
(7) ⁻ Simple homeostasis — simple Hopf: $-y^3 + (\lambda^2 - c)y$			

Blue (red) curves indicate stable (unstable) equilibria. Green curves indicate the minimum and maximum of stable limit cycles. Black curves indicate amplitudes of stable limit cycles. Homeostasis points are marked. Regions (6)(c) and (6)(d) were highlighted in the introduction (Fig. 3).

Table 6. (Continued)



Blue (red) curves indicate stable (unstable) equilibria. Green curves indicate the minimum and maximum of stable limit cycles. Black curves indicate amplitudes of stable limit cycles. Homeostasis points are marked. Regions (8)⁺ and (8)⁻(j) predict wide homeostatic plateaus in amplitude.

Table 6. (Continued)

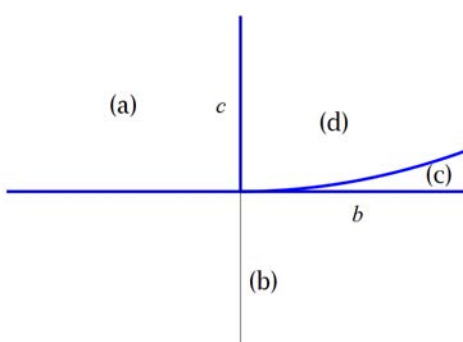
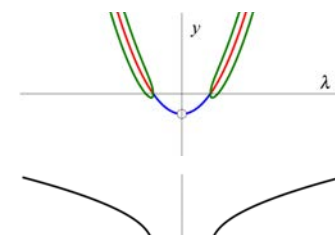
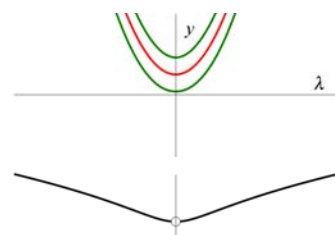
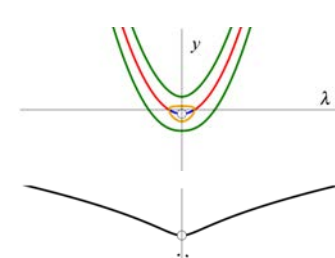
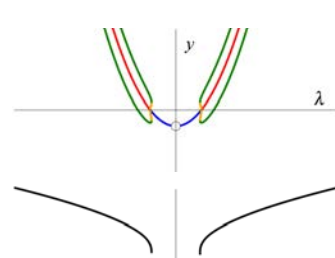
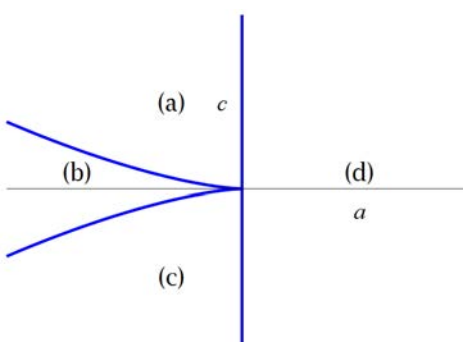
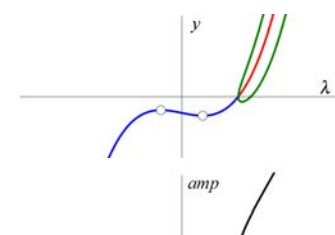
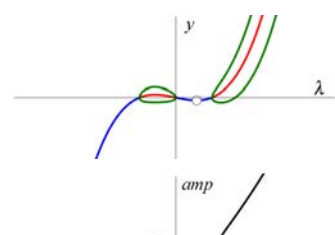
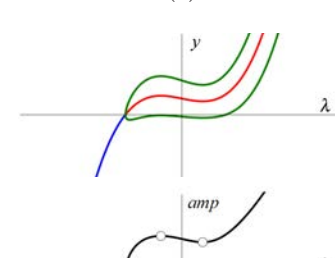
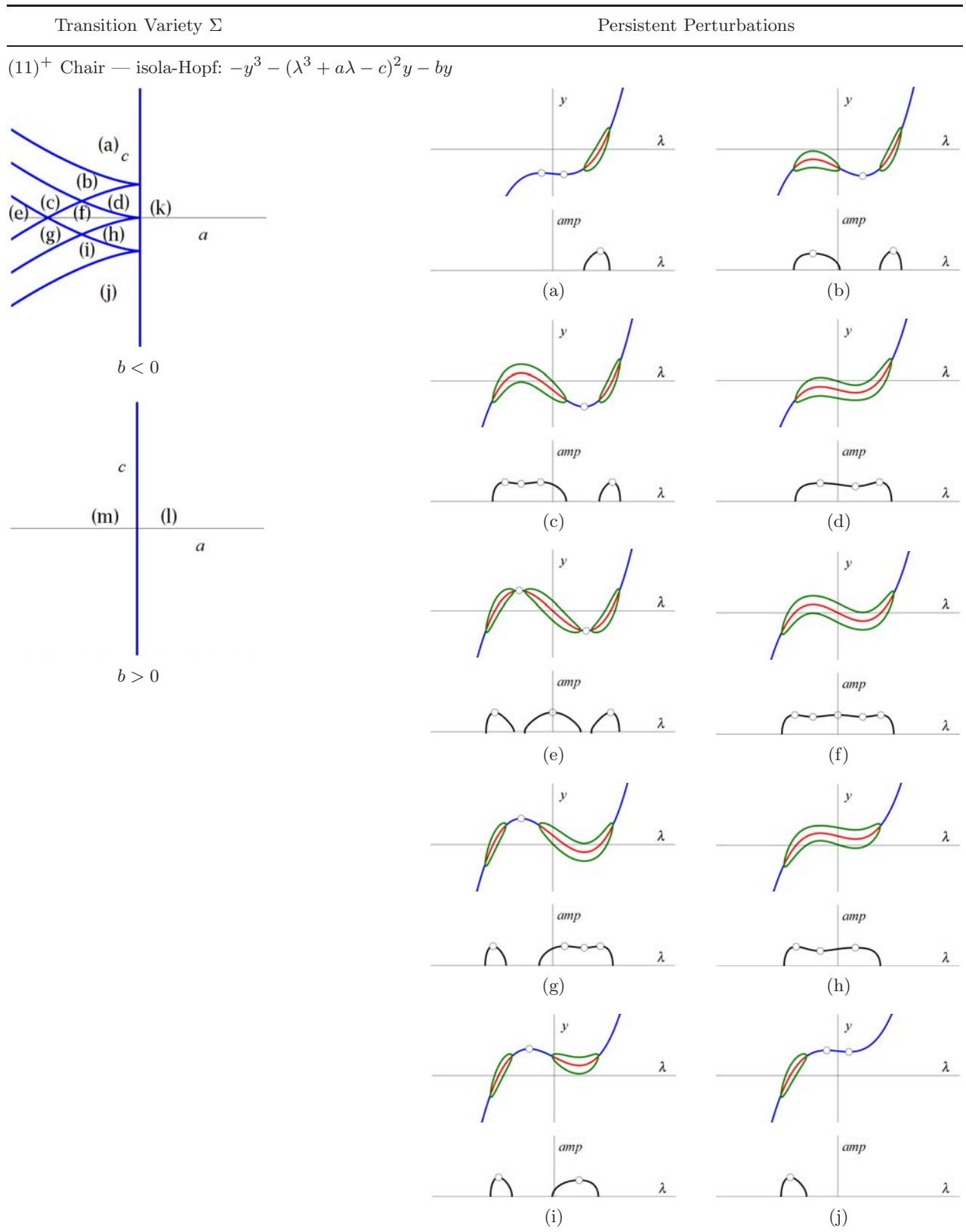
Transition Variety Σ	Persistent Perturbations			
(9) $-y^5 + (\lambda^2 - c)y + by^3$				
				
(10) Chair — simple Hopf: $-y^3 + (\lambda^3 + a\lambda - c)y$				

Table 6. (Continued)



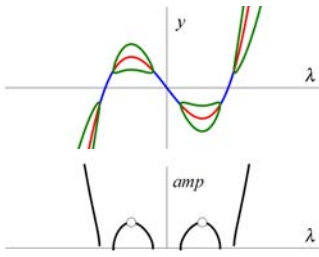
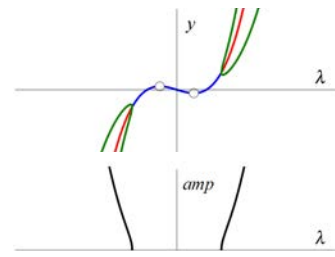
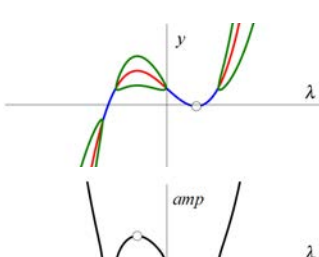
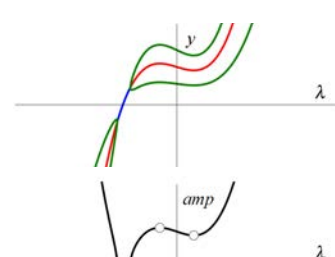
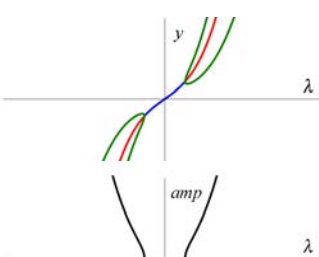
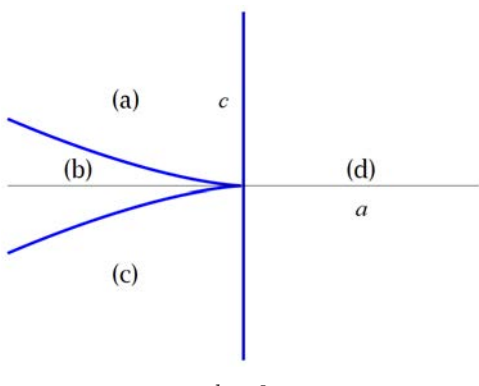
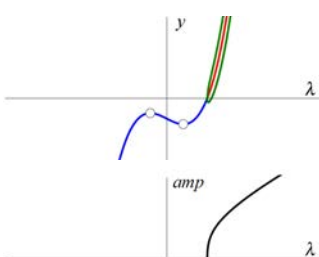
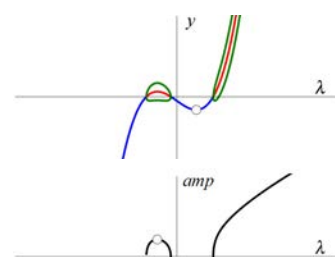
Blue (red) curves indicate stable (unstable) equilibria. Green curves indicate the minimum and maximum of stable limit cycles. Black curves indicate amplitudes of stable limit cycles. Homeostasis points are marked. Regions (11)⁺(f), (11)⁺(h), and (11)⁺(d) were highlighted in the introduction (Fig. 5).

Table 6. (Continued)

Transition Variety Σ	Persistent Perturbations		
(11) ⁻ $-y^3 + (\lambda^3 + a\lambda - c)^2 y + by$			
$b < 0$ $b > 0$ 			

Blue (red) curves indicate stable (unstable) equilibria. Green curves indicate the minimum and maximum of stable limit cycles. Black curves indicate amplitudes of stable limit cycles. Homeostasis points are marked. Regions (11)⁻(a)–(11)⁻(c) predict wide homeostatic plateaus in amplitude and period.

Table 6. (Continued)

Transition Variety Σ	Persistent Perturbations
(g)	
(h)	
(i)	
(j)	
(k)	
(12) $-y^5 + (\lambda^3 + a\lambda - c)y + by^3$	
 $b < 0$	 

Blue (red) curves indicate stable (unstable) equilibria. Green (orange) curves indicate the minimum and maximum of stable (unstable) limit cycles. Solid (dashed) black curves indicate amplitudes of stable (unstable) limit cycles. Homeostasis points are marked. Region (12)(h) predicts coexistence of homeostatic steady-states and homeostatic limit-cycles. Varying λ will cause switching between the two types of solutions.

Table 6. (Continued)

Transition Variety Σ	Persistent Perturbations	
 $b > 0$	 	

phenomena, we do not plot the period of limit cycle solutions. However, homeostasis points of the period which are inherited by x can be recovered by noting that these coincide with homeostasis points on the branch of unstable equilibria (see Fig. 5 for an example). We assume that $f_y < 0$ indicates a stable equilibrium.

Acknowledgments

We thank Mike Reed for many helpful conversations. The research of M. Golubitsky was supported in part by National Science Foundation Grant DMS-1440386 to the Mathematical Biosciences Institute.

References

- Antoneli, F., Golubitsky, M. & Stewart, I. [2018] “Homeostasis in a feed forward loop gene regulatory motif,” *J. Theoret. Biol.* **445**, 103–109.
- Bass, J. & Takahashi, J. S. [2010] “Circadian integration of metabolism and energetics,” *Science* **330**, 1349–1354.
- Dhooge, A., Govaerts, W., Kuznetsov, Y. A., Meijer, H. G. & Sautois, B. [2008] “New features of the software matcont for bifurcation analysis of dynamical systems,” *Math. Comput. Model. Dyn. Syst.* **14**, 147–175.
- Dibner, C., Sage, D., Unser, M., Bauer, C., d’Eysmond, T., Naef, F. & Schibler, U. [2008] “Circadian gene expression is resilient to large fluctuations in overall transcription rates,” *EMBO J.* **28**, 123–134.
- Donovan, G. M. [2018] “Biological version of Braess’ paradox arising from perturbed homeostasis,” *Phys. Rev. E* **98**, 062406.
- Duncan, W., Best, J., Golubitsky, M., Nijhout, H. & Reed, M. [2018] “Homeostasis despite instability,” *Math. Biosci.* **300**, 130–137.
- Golubitsky, M. & Schaeffer, D. G. [1985] *Singularities and Groups in Bifurcation Theory: Vol. I*, Applied Mathematical Sciences, Vol. 51 (Springer-Verlag, NY).
- Golubitsky, M. & Stewart, I. [2016] “Homeostasis, singularities, and networks,” *J. Math. Biol.* **74**, 387–407.
- Mulukutla, B. C., Yongky, A., Daoutidis, P. & Hu, W.-S. [2014] “Bistability in glycolysis pathway as a physiological switch in energy metabolism,” *PLoS One* **9**, 1–12.
- Reed, M., Best, J., Golubitsky, M., Stewart, I. & Nijhout, H. F. [2017] “Analysis of homeostatic mechanisms in biochemical networks,” *Bull. Math. Biol.* **79**, 2534–2557.

Appendix A

Reduction of System (4) to Eq. (5)

In the case of steady-state bifurcation we use the Lyapunov–Schmidt method to reduce (4) to a scalar equation. We show that the reduced equation preserves homeostasis points of a chosen state variable Y_k as well as the multiplicity and stability of solutions.

Consider the equation

$$F(Y, \mu, b) = 0 \quad (\text{A.1})$$

where $Y \in \mathbb{R}^n$, $\mu \in \mathbb{R}$ is a distinguished parameter, and $b \in \mathbb{R}^p$ is a vector of auxiliary parameters. We begin by explaining what we mean by Y_k homeostasis points. Suppose that $F = 0$ and $D_Y F$ is nonsingular at (Y_0, μ_0, b_0) . Then we may apply the implicit function theorem to obtain a function $Y(\mu, b) \in \mathbb{R}^n$ where, near (μ_0, b_0) , $F(Y(\mu, b), \mu, b) = 0$. However, we will soon assume that F undergoes a bifurcation, so it is possible that there is another value of Y , say \tilde{Y}_0 , so that $F(\tilde{Y}_0, \mu_0, b_0) = 0$. For this reason, it will be useful to specify the value of Y when describing the homeostasis point.

Definition A.1. The function $\rho : \mathbb{R} \times \mathbb{R} \times \mathbb{R}^p \rightarrow \mathbb{R}$ has a homeostasis point at (ρ_0, μ_0, b_0) if $\rho(\mu_0, b_0) = \rho_0$ and $\rho_\mu(\mu_0, b_0) = 0$.

A.1. Derivation of the reduction

Suppose F undergoes a simple 0-eigenvalue bifurcation at $(Y, \mu, b) = (0, 0, 0)$. We perform a Lyapunov–Schmidt reduction on F at the bifurcation point to get a scalar function, $f : \mathbb{R} \times \mathbb{R} \times \mathbb{R}^p \rightarrow \mathbb{R}$ so that, locally, solutions to $f(y, \mu, b) = 0$ are in one-to-one correspondence with solutions of (A.1). Let $L = (D_Y F)_{(0,0,0)}$. Lyapunov–Schmidt reduction requires making a choice of complementary subspaces M to $\ker(L) = \mathbb{R}\{v_0\}$ in \mathbb{R}^n and N to $\text{range}(L) = \mathbb{R}\{v_0^*\}$ in \mathbb{R}^n . In order for Lyapunov–Schmidt reduction to preserve homeostasis of the k th coordinate in the original equation $F = 0$ to the reduced equation $f = 0$, we must also assume the nondegeneracy condition on L at the origin

$$\langle v_0, e_k \rangle \neq 0$$

or $e_k \notin (\ker L)^\perp$. It follows that we can split the domain of L via $\mathbb{R}^n = \ker L \oplus M$ by choosing $M = \text{span}\{e_i \mid i \neq k\}$. We additionally split the codomain

of L via $\mathbb{R}^n = \text{range } L \oplus N$. The choice of N is arbitrary.

Let E denote projection onto $\text{range } L$ with $\ker E = N$. We may solve $F(Y, \mu, b) = 0$ by simultaneously solving

$$\begin{aligned} EF(Y, \mu, b) &= 0 \\ (I - E)F(Y, \mu, b) &= 0 \end{aligned}$$

where I denotes the $n \times n$ identity.

The reduction continues by decomposing Y as $Y = v + w$ where $v \in \ker L$ and $w \in M$. Applying the implicit function theorem to $EF(v + w, \mu, b) = 0$ yields $w \equiv w(v, \mu, b)$. Define $\phi : \ker L \times \mathbb{R} \times \mathbb{R}^p \rightarrow N$ by $\phi(v, \mu, b) = (I - E)F(v + w(v, \mu, b), \mu, b)$. So that our reduction preserves stability, we require $\langle v_0, v_0^* \rangle > 0$, where $\langle \cdot, \cdot \rangle$ is the standard inner product on \mathbb{R}^n . This is called a consistent choice of v_0 and v_0^* (see [Golubitsky & Schaeffer, 1985] for more details). The reduction is now given by

$$f(y, \mu, b) = \langle v_0^*, \phi(yv_0, \mu, b) \rangle. \quad (\text{A.2})$$

Note that if (y, μ, b) solves $f(y, \mu, b) = 0$ then Y in the corresponding solution of $F(Y, \mu, b) = 0$ can be recovered via

$$Y = yv_0 + w(yv_0, \mu, b). \quad (\text{A.3})$$

A.2. Preservation of the desired properties

Solutions of $f = 0$ and $F = 0$ are in one-to-one correspondence, so multiplicity of solutions is automatically preserved. Let $\lambda_1, \dots, \lambda_n$ denote the eigenvalues of $D_Y F_{(0,0,0)}$ with $\lambda_1 = 0$. Note that we have assumed $\text{Re}(\lambda_i) \neq 0$ for $i \neq 1$. The following

proposition shows that the stability of solutions is preserved if we make an additional assumption on λ_i .

Proposition 3. Suppose $\text{Re}(\lambda_i) < 0$ for $i \neq 1$. Then the equilibria of $\dot{Y} = F(Y, \mu, b)$ corresponding to a solution, (y, μ, b) , of $f(y, \mu, b) = 0$ is asymptotically stable if $f_y(y, \mu, b) < 0$ and unstable if $f_y(y, \mu, b) > 0$.

Proof. See Chapter 1, Theorem 4.1 of [Golubitsky & Schaeffer, 1985]. ■

Now, given $f(y_0, \mu_0, b_0) = 0$ and $f_y(y_0, \mu_0, b_0) \neq 0$ we may apply the implicit function theorem to obtain a curve $y(\mu, b)$ where $f(y(\mu, b), \mu, b) = 0$ and $y(\mu_0, b_0) = y_0$. The one-to-one correspondence of f and F gives a corresponding curve of equilibria, $Y(\mu, b)$ with $Y(\mu_0, b_0) = Y_0$.

Definition A.2. If y has a homeostasis point at (y_0, μ_0, b_0) if and only if Y_k has a homeostasis point at $((Y_0)_k, \mu_0, b_0)$ where Y_0 is the corresponding solution to y_0 , then f is Y_k homeostasis preserving.

Proposition 4. f is Y_k homeostasis preserving.

Proof. Suppose $y(\mu, b)$ satisfies $f(y(\mu, b), \mu, b) = 0$. The corresponding solutions to $F = 0$ are given by (A.3):

$$Y(\mu, b) = y(\mu, b)v_0 + w(yv_0, \mu, b).$$

However, $w(yv_0, \mu, b) \in M$ so $w_k(y(\mu, b)v_0, \mu, b) \equiv 0$ and we have $Y_k(\mu, b) = y(\mu, b)(v_0)_k$. Therefore $(Y_k)_\mu(\mu, b) = y_\mu(\mu, b)(v_0)_k$ and f preserves Y_k homeostasis. ■